Use of Conducting Electroactive Polymers for Drug Delivery and Sensing of Bioactive Molecules. A Redox Chemistry Approach

Jean-Michel Pernaut*

Departamento de Química, ICEX CP702, Universidade Federal de Minas Gerais, 31270-901, Belo Horizonte/MG, Brazil

John R. Reynolds*

Department of Chemistry, Center for Macromolecular Science and Engineering, University of Florida, Gainesville, Florida 32611

Received: December 6, 1999; In Final Form: January 31, 2000

We have examined the properties of polypyrrole (PPy) as a model electroactive membrane which can simultaneously serve as a medium sensing, and bioactive molecule releasing, material using optical spectroscopic, potentiometric, and conductometric methods. In particular, PPy membranes can sense hydrazine in aqueous solution with linear logarithmic potentiometric and conductometric responses between 10^{-4} and 10^{-1} M. The sensing properties of the PPy membranes are discussed in terms of both its redox properties and specific acid−base behavior. Adenosine triphosphate (ATP) has been used as a model drug which is easily loaded into PPy during electrochemical synthesis. ATP release processes from PPy/ATP membranes have been studied spectroscopically using electrochemical and chemical triggering. Electrochemical triggering allowed ATP to be delivered with a variety of release profiles and adjustable rates (up to 20 μg cm^{-2} min^{-1} for a 10 μm thick membrane). The mass transfer through the membranes has been successfully treated using a simple diffusion model ($D \sim 5 \times 10^{-9}$ cm^2 s^{-1}) and discussed with regards to the polymer's structure and potential drug delivery device applications. Hydrazine (0.1 M) and alkaline medium (pH 12) have been used as chemical triggers for ATP release from PPy/ATP membranes. The amount of ATP released was reduced relative to the electrochemically released amount due to inhibited diffusion of reagents into the membranes. The release profiles have been established and demonstrate the viability of a controlled-delivery device using conducting polymers.

Introduction

Recently there has been a significant effort directed to finding new drug release systems in which bioactive molecules contained in a reservoir can be supplied to a host system while controlling the rate and period of delivery.[1] The optimum mode of administration would be achieved if the drug was delivered to a precise region of the body where it is physiologically required. In addition, the system should be able to sense some chemical species in the physiological medium (e.g., pH or concentration of a given analyte) and self-regulate its delivery (chemical triggering), or it could be controlled using an external trigger.

Polymers have proven especially useful materials for drug carriers since they can be easily processed and their physical and chemical properties tuned via molecular architecture.[2] Conducting electroactive polymers (CEPs) have been considered for drug delivery due to their unique redox properties which allow controlled ionic transport through the polymeric membrane. Electrochemical switching of the polymer is accompanied by the movement of counterions, so-called dopant ions, in and out of the membrane for charge balance.[3] On the basis of these properties, a variety of anions including salicylate and ferrocyanide,[4] glutamate,[5] and ATP[6] have been electrostatically entrapped into conducting polymer membranes and released during reduction. Furthermore, by entrapping large anionic dopants inside the membrane, cations have been released during oxidation of the polymer; such processes included the release of protonated dopamine.[7] Finally, conducting polymer membranes have been studied as ion-gate and permselective membranes where it was shown that morphology and permeability could be adjusted according to the redox state of the polymer.[8]

Conducting polymers have also been used for chemical and biological sensing in a number of applications and device configurations.[9] Efforts have been made to develop selective and sensitive chemical sensors and in particular biosensors which were achieved by immobilizing a biological element (enzyme, antibody, or receptor).[10] Chemical sensors are classified according to the transducer type,[11] as represented by the electrochemical sensors (amperometric, potentiometric, or conductometric) which are a subject of this work. Among the electrochemical sensors based on conjugated polymers, the first and simplest sensors were based on the undoped polymer exposed to the dopant vapor.[12] A large number of different kinds of sensors have been described, including gas sensors (NH_3,[13] SO_2,[14] etc.), ion sensors (Cl^-,[15] pH,[16] etc.), and biosensors (glucose,[17] proteins,[18] DNA,[19] etc.).

The aim of this work was to study the ability of a conducting polymer to sense a chemical species in solution (chemical sensing) and to subsequently release another chemical substance

* For correspondence: E-mail reynolds@chem.ufl.edu and jmpe@dedalus.lcc.ufmg.br.

10.1021/jp994274o CCC: $19.00
Published on Web 03/30/2000

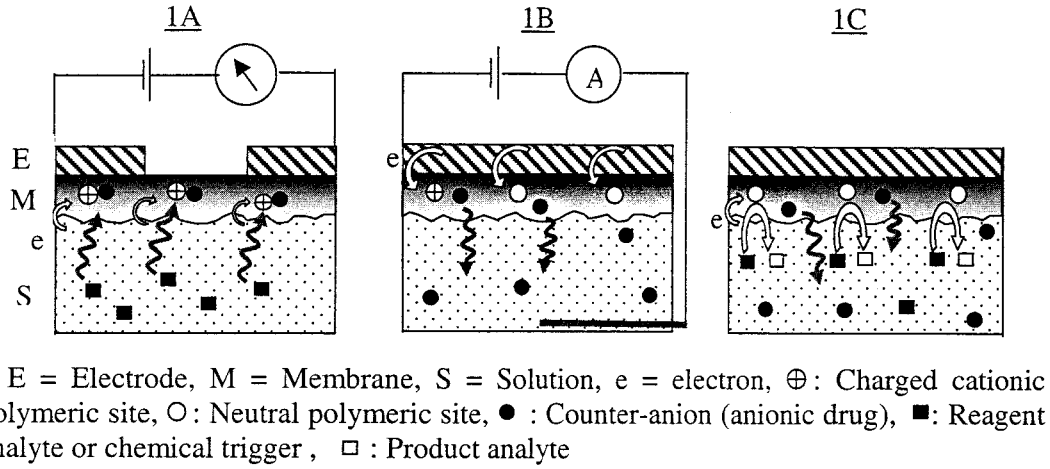

Figure 1. Schematic representations of the principles of (A) chemical sensing of an analyte (■), (B) electrochemically triggered release of a drug (●), and (C) chemically triggered release of a drug by a reactive analyte (■) for a device consisting of a CEP membrane (M) loaded by an anionic drug and supported on an electrode (E).

(drug) as a function of the concentration of the sensed species (chemical triggered release). In addition, the amount of the drug released could be controlled by means of an external action (electrochemically triggered release). The system polypyrrole (PPy)/adenosine triphosphate (ATP) was chosen as a conducting polymer/anionic drug model to determine the electrochemical parameters that control the sensing and releasing functions and to build a self-regulated model based on the release of ATP by chemical triggers. The system consisted of a polymer membrane (the terminolgy membrane is preferred here to film due to the ability of the conducting polymer to pass ions) on a conducting substrate (delivery unit) in contact with a solution or liquid electrolyte (host unit). The redox potential of the polymer can be used for sensing interactive species[10b] while another key property for both the sensing and releasing functions is the charge doping level of the polymer. This electrochemical property can be directly measured by chronocoulometry (or by integrating the current from slow scan rate cyclic voltammetry). However, due to the contribution from double layer charging to the overall electrical charge injected in the polymer, the charge doping level changes are better determined indirectly by measuring the electrical potential of the membrane (E), the electrical conductivity of the membrane (σ), or the optical absorbance of the polymer (A_P). Any of these properties (E, σ, or A_p) can be used as an indicator of drug level in the membrane and to sense a chemical species (analyte) present in the contact solution providing this species is able to chemically change the charge level of the polymer; this may be accomplished by either redox or acid−base mechanisms.

In this paper, we present a fundamental approach to the sensing and releasing properties of CEPs. Neither selectivity nor optimal sensitivity of the systems was sought, but our efforts were rather directed to understanding of the electrochemistry involved in these redox processes. The three basic functions studied in this work—chemical sensing, electrochemically triggered release, and chemically triggered release—are shown schematically in Figure 1. The fact that such different release mechanisms can be exploited in a single material is due to the unique chemical and electrochemical properties of CEPs.

PPy ($(C_4H_2NH)_n$) was chosen as a model conducting polymer due to its well-known aqueous electrochemistry and acid−base properties,[20] allowing it to be considered in a number of applications as a biomaterial.[21] It should be noted that other polymer derivatives could be of particular interest for their different chemical reactivities or accessible redox potential ranges. ATP is a biological molecule indispensable for cellular energy transfer, and it has also been studied for cardiovascular therapeutic applications.[22] To model the sensing function of the polymer as a stimuli-sensitive drug delivery system, hydrazine (N_2H_4) was chosen as the principal chemical trigger. N_2H_4 is a reductant of interest in both the chemical and pharmaceutical industry. As its vapors are toxic, a number of gas sensors have been developed including simple chemiresistors based on conducting polymers.[23] On the other hand, to operate our polymeric drug delivery system in a biomimetic context, the bioreductant dithiothreitol ($HSCH_2CH(OH)CH(OH)CH_2SH$ = DTT) was also utilized; DTT is important biologically due to its implication in thiol/disulfide interchange reactions, and it is thermodynamically able to reduce oxidized PPy.[24] Finally, pH effects were studied as bioenvironmental factors that could affect the redox state of PPy. Previous studies of PPy have shown that the conductivity could be monitored through several pH decades.[25] In physiological systems, pH variations are limited from 2 to 8 (between gastric mucosa and Ileum[1]), conditions under which PPy remains electroactive. In this paper, we first address the electrochemical properties of the PPy/ATP redox system, and subsequently the sensing properties of PPy/ATP membranes toward N_2H_4, DTT, and pH are examined using potentiometry, conductometry, and optical spectroscopy. The electrochemically triggered release of ATP was then analyzed by spectroscopy, and the mass transfer was quantified using an appropriate diffusion model. Finally, the chemically induced release of ATP is reported.

Experimental Section

Chemicals. Pyrrole (Aldrich) was passed over neutral alumina until colorless before use. ATP disodium salt (Sigma Chemical), $NaClO_4$, NaCl, DTT, and N_2H_4 (Aldrich) were used without further purification. For the sensing measurements, 11 M N_2H_4, 2 M DTT, and 10 M NaOH concentrated solutions were used to avoid significant volume changes during additions.

Electrochemistry. The electrochemical cell consisted of a 5−20 mL glass flask, Pt button (0.02 cm^2), ITO (Delta Technologies, R_s < 10 Ω/□, exposed area 0.15 cm^2) or Interdigitated Microelectrodes (IME Pt-1050-FD-U Abtech Technologies, Pt area 0.05 cm^2) working electrodes (WE), a Pt plate as a counter electrode (CE), and an $Ag/AgCl/KCl_{sat}$ reference electrode (RE); all potentials in the text are referred to this electrode (E_{RE} = 200 mV/NHE). The electrochemical

apparatus was an EG&G potentiostat/galvanostat model 273A. PPy/ATP membranes were prepared either potentiostatically (0.5−1.0 V vs Ag/AgCl) or galvanostatically (0.1−10 mA cm^{-2}) using 0.25 M pyrrole and 20 mM ATP in doubly distilled water. The pH was adjusted to 6.2 as we found that in these conditions the membranes were more adherent on the interdigitated microelectrodes (IMEs) and yielded more stable electrochemical properties. After electrosynthesis, the membranes were thoroughly rinsed with water and placed in a given aqueous electrolyte (adjusted to pH 6.2) of 0.02 M ATP, 0.1 M NaCl, or 0.1 M NaH_2PO_4 buffer free from monomer. All solutions were degassed with argon prior to use, and all experiments were carried out at room temperature (22 ± 2 °C).

Electrosynthesis and cyclic voltammetry experiments were performed without agitation while stirred solutions were used for potentiometric, conductometric, and spectrophotometric experiments unless specified in the text.

The membrane thickness was determined from a calibration curve obtained by ex-situ measurements on dry membranes deposited on ITO substrates using a 3030 Dektak profilometer. The average of several measurements done on a series gave the relation L (μm) = $K_L Q_p$ (C cm^{-2}) with $K_L = 4.5 \pm 0.5$ μm C^{-1} cm^2 where Q_p is the charge passed during electropolymerization. On the other hand, knowing the membrane density and the doping level (x) and assuming a quantitative polymerization yield, it is possible to calculate the membrane thickness from Q_p.[26] The membrane density was estimated by measuring its flotation density in standard organic solvents. Independent of synthesis conditions, the apparent density of PPy/ATP membranes was determined to be 1.50 ± 0.05 g cm^{-3} (equilibrium in $CDCl_3$). Using a value of $x = 0.25$ for the doping level of PPy^{x+} $(ATP^{3-})_{x/3}$ (see electrochemical properties in the next section), the relation L (μm) = $3.3Q_p$ C cm^{-2} was determined. The lower value of the electrochemically measured K_L suggested that the geometric density of this membrane could be as low as 1.1 g cm^{-3}. The membrane thickness was fixed at 10 μm via profilometry for this study unless specified in the text. The maximum charge concentration in the polymer membrane (P^*) was calculated from the doping level ($P^* = x/(2 + x)FK_L$, where F is the Faraday constant) and was 2.5 M using $K_L = 4.5$ μm C^{-1} cm^2.

In-Situ Conductivity. As this work was directed to measuring conductometric properties, it was important to develop a reliable method to measure the in-situ conductivity changes of the polymeric membranes in the electrolytes. The IME arrays used consisted of two buses of 50 platinum lines separated by 10 μm spaces. The IME's were first electrically characterized using a frequency analyzer HP model 4192A (range $10-10^6$ Hz) and Fisher Scientific conductivity calibration standards (σ_S = $10^{-1}-10^{-5}$ S cm^{-1}). The lead (R_L) and solution (R_S) resistances were respectively identified as the high- and low-frequency resistances, and the cell constant of the IME's for a liquid electrolyte was determined as $K_C = R_S\sigma_S$. After cleaning with acetone, cathodizing in H_2SO_4 0.5 M (−0.3 V for 5 min), and activation in *piranha* solution (H_2SO_4: H_2O_2 4:1) for 30 s, the electrical parameters (R_L, K_C) of the electrodes were determined prior to polymerization experiments ($R_L = 50-150$ Ω and $K_C = 0.05-0.075$ cm^{-1}). After electrodeposition of a polymer membrane with a thickness larger than 5 μm (required for IME connection), the membranes electrical resistance was measured using two potentiostats according to a procedure derived from that introduced by Wrighton et al. [27] In this setup, the WE output of the first potentiostat was connected to one IME channel to control the doping level of the polymer by means of a gate potential (V_G) which was applied vs RE. The second potentiostat was used in a two-electrode configuration where the WE was connected to one channel and the CE and RE were both connected to the other. The electrical resistance of the polymer was determined by recording the current flowing between the channels (I_D) when a small offset potential was applied (V_D) under the form of a potential sweep or step, at pseudo-equilibrium ($|I| < 0.5$ μA): $R = V_D/I_D$. Linearity remained up to ±100 mV, but offset potentials lower than 50 mV were preferred for long time experiments. Since only relative changes were important for the sensing measurements, results were presented either in terms of I_D (which is proportional to the conductivity) or in terms of normalized conductivity which included the correction due to R_L ($\sigma_N = (R_{max} - R_L)/(R - R_L)$). To get an estimation of the conductivity of the oxidized polymer, the relation $\sigma = K_C/(R - R_L)$ was used as an approximation for the 10 μm thick membranes since for thicker films the resistance of the IME's tended to R_L as R is reduced.

For conductometric (or potentiometric) sensing experiments, starting from a 0.1 M NaCl or phospate buffer (pH sensing experiments) solution, small amounts of the chemical trigger were titrated into the solution under continuous stirring, and the I_D (or open circuit potential E_{oc}) was monitored versus time (detection via chronoamperometry or chronopotentiometry). Equilibrium values were measured after a current (or potential) plateau was reached.

Spectrophotometry. For the sensing experiments, the absorbance changes of thin PPy/ATP membranes (0.1−0.5 μm) deposited on ITO and placed in a UV−vis cuvette cell were monitored in situ using a Cary 5E UV−vis spectrophotometer. For the release experiments, ATP concentration changes in the electrolyte in contact with a 10 μm thick PPy/ATP membrane deposited on ITO were monitored in situ under constant stirring by measuring the absorbance ($\lambda_{max} = 260$ nm) using an optical fiber equipped Spectra Instruments Inc. model 440 CCD spectrophotometer.

Results and Discussion

Review of Electrochemical Properties of PPy/ATP. To use the redox-controlled sensing and releasing properties of PPy/ATP as a potential drug delivery system, it is necessary that the polymer exhibits a stable and reproducible electrochemical response under the conditions to which it will be exposed. The electrochemical behavior of PPy/ATP has been previously reported and shows varied features according to the synthesis conditions and cycling electrolyte.[28] Examining the CV of a PPy/ATP membrane in an ATP aqueous electrolyte, both monomer and ATP concentrations in the synthesis solution could be varied between 0.05 and 0.5 M without significant changes in the CV of the resultant polymer. The pH-controlled ionization state of the ATP ion incorporated into the membrane during synthesis does play a role, as the CV is unstable in ATP electrolyte solutions when the synthesis pH was below 4. On the other hand, as shown by a typical stable and reproducible cyclic voltammogram (CV) in Figure 2A using NaCl as an electrolyte, PPy/ATP exhibits good cycling stability independent of synthesis pH when the polymer is studied in an electrolyte containing a smaller monoanion.

Previous results show the diffusion of ATP to be a slow process; the sodium cation is incorporated during the first few cycles, and subsequently anion exchange takes place.[6] Now we find that the electrochemically cycled charge (determined by anodic current integration from slow scan CV) was small in ATP electrolyte ($x \sim 10\%$ or 0.1 e^-/pyrrole ring) as compared

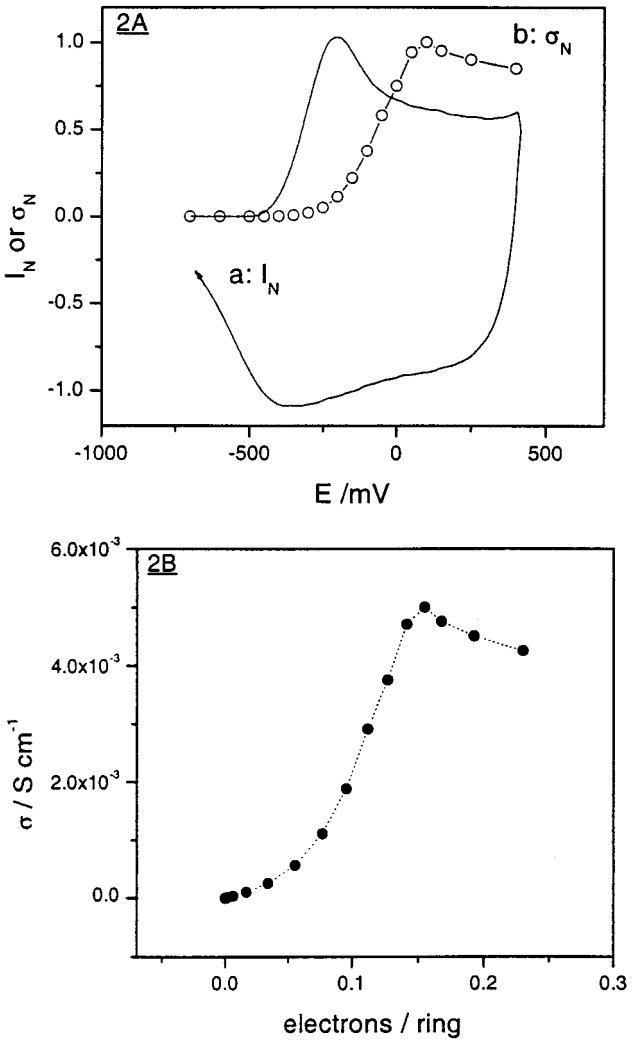

Figure 2. (A) CV (curve a shown as normalized current I_N) of a 10 μm thick PPy/ATP membrane cycled in 0.1 M NaCl at 5 mV s^{-1} and normalized in-situ conductivity (σ_N) as a function of potential (curve b). (B) In-situ conductivity as a function of electrochemical doping charge (expressed as e^-/ring = x).

to NaCl electrolyte ($x \sim 25\%$). This is likely due to the better effectiveness of Cl^- as an electrochemical dopant as compared to K^+ in PPy/ATP. Concerning the electrosynthesis mode, a low polymerization rate (<1 mA cm^{-2}) led to a more dense and homogeneous membrane, while irregular surfaces and even macroscopic dendrites were formed at higher rates (>5 mA cm^{-2}). Important for later considerations using IMEs, both platinum (disk and IME) and ITO substrates offered similar CV results for 10 μm thick membranes.

As previously mentioned in the Introduction, the conductivity (σ) of the polymer membrane is a function of the electrochemical charge x and can be used to sense a species that can alter x chemically (chemoresistive sensor).[9b] To obtain an understanding of the redox state on charge transport properties, we studied the conductivity as a function of doping charge by controlling the applied potential. A typical $\sigma-E$ conductivity curve is presented in Figure 2A (curve b), and the $\sigma-x$ relationship deduced is shown in Figure 2B. The $\sigma-x$ relationship exhibits a sigmoidal shape with an onset of conductivity corresponding to a charge threshold about 0.05 e^-/ ring (or $x = 5\%$) followed by a linear increase, and finally a pseudo-plateau was reached at about $x = 15\%$ (note that $x = 23\%$ at +0.4 V). While it should be noted that there may be charge inhomogeneity in the membrane, and possibly specific interactions of dopants with the charge carriers,[29] for the purpose of this study the conductivity of the membrane was considered to be an indicator of the doping level. It is also worth noting in Figure 2B that the in-situ calculated σ_{max} (solvated state) was about 5×10^{-3} S cm^{-1}, i.e., 20 times less than the ex-situ dry state conductivity (0.1 S cm^{-1}) as expected. Nevertheless, this conductivity is at a satisfactory level for a chemoresistive application.

Study of Chemical Sensing of PPy/ATP. Above, we have introduced the possibility of using the potential, the conductivity, and the absorbance of the PPy membrane to sense a chemical species that can reduce the electrochemical charge of the polymer. In this section, these properties are applied to reductants (N_2H_4 and DTT) and to alkaline solutions.

Potentiometric Sensing. The equilibrium potential was considered as the open-circuit potential of the electrode after equilibrium had been reached. For an electroactive polymer membrane immobilized on an inert electrode, this potential is related to the charge or redox state of the polymer.[26,30] As an approximation, the redox reaction (eq 1) is equivalent to a monoelectronic transfer between four charged pyrrole rings ($x \sim 0.25$ e^-/ring), represented here as PH^+ (where P accounts for four rings and H is the hydrogen bound to the oxidized pyrrolylium nitrogen), and four neutral rings (PH) (see the structures in Figure 3).

$$PH^+ + 1e^- \rightleftarrows PH \qquad (1)$$

For a reversible redox reaction, we have at equilibrium using the Nernst equation:

$$E = E^{\circ\prime} + RT/F \ln\{([P^*] - [PH])/[PH]\} \qquad (2)$$

where $E^{\circ\prime}$ is the formal potential of the reaction, and [P*] ([P*] = [PH^+] + [PH]) is the total species concentration equal to the maximum charge concentration which was estimated to be 2.5 M (see Experimental Section).

Reduction by Hydrazine (N_2H_4). The interaction of N_2H_4 with a CEP leads to the neutralization of active sites of the polymer, mainly by chemical reduction (N_2H_4 oxidation), although oxidized pyrrolylium nitrogen deprotonation cannot be ignored as N_2H_4 is basic.[31] The oxidation process of N_2H_4 by a conducting polymer is a heterogeneous process and probably resembles, to some extent, the electrooxidation of N_2H_4 on a metal electrode. In this instance, after N_2H_4 adsorption, slow mono-electronic and fast three-electronic steps have been identified.[32] The overall scheme is

$$(N_2H_4)_{ads} \rightarrow N_2 + 4H^+ + 4e^- \qquad (3)$$

We studied the electrooxidation of N_2H_4 in H_2O, with 10^{-2} M N_2H_4 and 10^{-1} M NaCl on a Pt electrode by cyclic voltammetry between −1100 and +500 mV. Two processes could be clearly identified on the CV at −900 and −600 mV. In the case of a polymer-coated electrode with a unity partition coefficient of N_2H_4 between membrane and solution, assuming complete oxidation of the reductant ($4e^-/N_2H_4$) and no pH interference, eq 2 can be rewritten as

$$E = E^{\circ\prime} + 2.3RT/F \log\{(10 - [N_2H_4])/[N_2H_4]\} \qquad (4)$$

A typical chronopotentiogram, corresponding to the open-circuit potential response to incremental addition of N_2H_4, is shown in Figure 4A, from which a potentiometric detection curve was derived (curve a, Figure 4B). We observed that, after the first reduction steps ($E_{oc} < -100$ mV), the response time of thin PPy membranes was quite fast, which suggested an easy

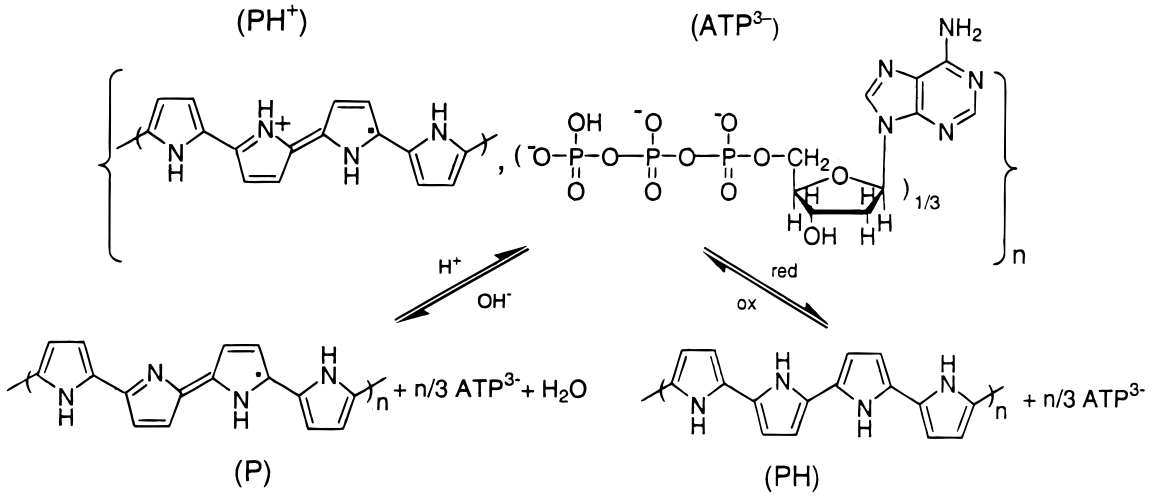

Figure 3. Equilibrium reaction schemes proposed for conversion between oxidized polaronic PPy (PH^+, $ATP^{3-}_{1/3}$), neutral reduced (chemically or electrochemically) aromatic PPy (PH), and neutral deprotonated quinoidal PPy (P).

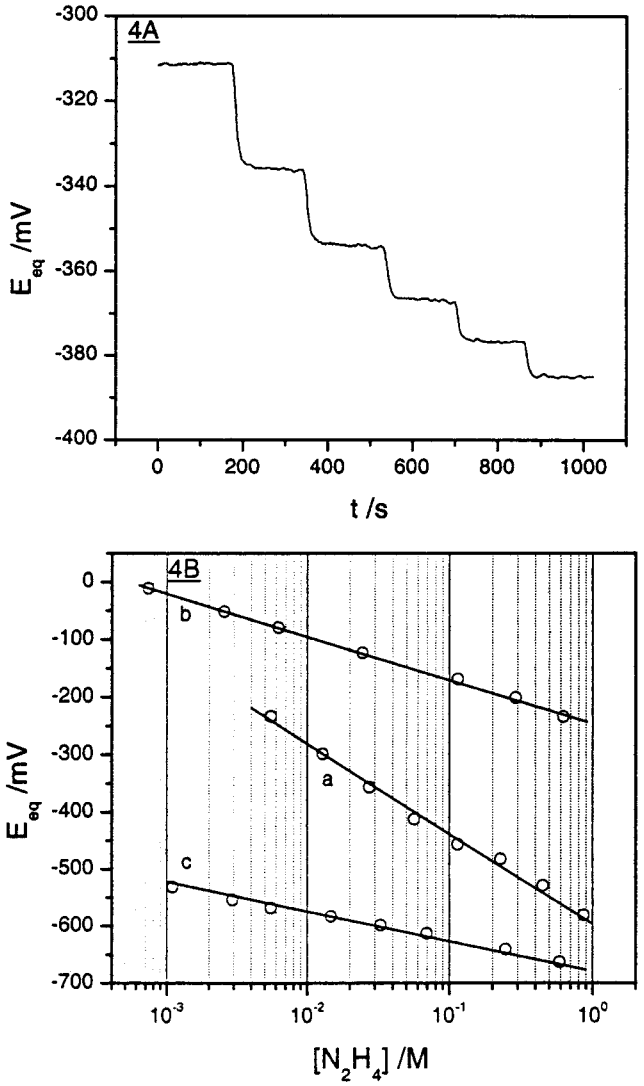

Figure 4. (A) Equilibrium potential as a function of time for a 1 μm thick PPy/ATP membrane (supported on a 0.02 cm^2 Pt disk exposed to a H_2O/0.1 M NaCl solution) with successive increments (5.5 mM) of N_2H_4. (B) Potentiometric titration of (a) PPy/ATP (5 μm)-coated platinum electrode, (b) bare platinum electrode, and (c) bare ITO electrode with N_2H_4.

diffusion and reaction of N_2H_4 inside the membrane (Figure 4A). Applying the results of curve a in Figure 4B to eq 4 gave approximately −600 mV for $E^{\circ\prime}$ (apparent $E^{\circ\prime}$ from CV is −300 mV) and more than 120 mV/decade for the slope.

The redox process of PPy was found to be super-Nernstian, in agreement with the nonideal electrochemical behavior of PPy for which two electronic steps, coupled with large interaction potentials, should be considered.[33] In terms of N_2H_4 detection, these experiments were not optimized to measure the sensitivity limit, but the response of N_2H_4 was examined between 10^{-4} and 1 M. A linear regression analysis performed on a series of several experiments yielded an average slope of -130 ± 15 mV/decade of concentration, with a correlation coefficient of $R > 0.995$. Using smaller gap IME's (5 μm) with a thinner membrane would increase the sensitivity of the polymer sensor.

We also checked the capacity of bare platinum and ITO electrodes to potentiometrically sense N_2H_4 in the H_2O/0.1 M NaCl medium. Again, a good linearity was observed with log $[N_2H_4]$ between 10^{-3} and 1 M ($R > 0.997$), but the reproducibility was generally poor due to difficulties in obtaining reproducible Pt and ITO surfaces. Typical potentiometric responses are shown in Figure 4B for Pt (curve b, 50 mV/decade) and ITO (curve c, 70 mV/decade). This quasi-Nernstian behavior was attributed to the reduction of surface oxides by N_2H_4. These results indicate the polymer's response to be more reproducible, as it provides a higher exposed surface area than either Pt or ITO.

Reduction by Dithiothreitol (DTT). The electrochemical behavior of DTT in H_2O, 0.1 M NaCl (pH∼ 6.5) on Pt was first investigated by 50 mV s^{-1} CV, and a two-step irreversible oxidation process ($E_{pa1} = 250$ and $E_{pa2} = 775$ mV), followed by an irreversible reduction peak at −550 mV, was observed, sweeping anodically and cathodically, respectively. Note that the estimated formal redox potential of DTT has been reported to be −535 mV at pH = 7.[24] The reduction of oxidized PPy/ATP thin membranes, deposited on platinum, by DTT was studied using potentiometry. The potential changes are significantly slower than those observed using N_2H_4 (between 20 and 30 min) which suggested a slower kinetics of the reduction process and/or DTT diffusion through the membrane. In addition, the overall potential change observed, even when using large amounts of DTT, was relatively small. This is likely due to the chemical blocking effect of DTT on a platinum surface.[34] Examining the potential changes as a function of DTT concentration between 0.01 and 1 M gives a linear correlation with a potential of −60 mV obtained for [DTT] = 1 M. Interestingly,

the same value was extrapolated from experiments carried out on bare platinum. These experiments suggest that the same surface electrode process was controlling the potential in this concentration range, probably due to formation of stable metal−thiolate complexes.[34]

No reliable potentiometric response could be obtained with DTT on either glassy carbon or ITO surfaces in any electrolyte concentration or convective regime, due to electrode potential instability and the slow kinetics involved in these processes. Finally, attempts to obtain a better response using a polymer with a higher redox potential (e.g., ATP-doped poly(pyrrole/*N*-methylpyrrole) copolymer) were not successful, since the most likely useful copolymers (having a high fraction of *N*-methylpyrrole) were not sufficiently stable in standard NaCl electrolyte.

pH Effect. It has been shown in previous work that oxidized polypyrrole could be reversibly cycled between a conducting and a nonconducting state by sequential base and acid treatments.[25] Although some authors have proposed that the decrease of conductivity upon alkaline treatment was due to nucleophilic attack of OH^- at the β-position of pyrroles,[35] it seems more reasonable that this treatment results in the deprotonation of the nitrogen atom of pyrrole and subsequent neutralization of the charge carriers present in the polymer,[36] as shown in Figure 3.

Furthermore, it has also been proposed that as-prepared PPy membranes, exposed to aqueous nonbuffered solutions, could undergo an additional protonation similar to that produced by strong acid treatment.[36b] This led to the consideration of two proton transfers associated with the nitrogen sites to account for the acid−base properties of PPy,[20,36b] as described below:

$$PH^{2+} \rightleftarrows PH^{+} + H^{+} \quad (pK_a \sim 2-4) \tag{5}$$

$$PH^{+} \rightleftarrows P + H^{+} \quad (pK_a \sim 9-11) \tag{6}$$

The open-circuit potential of oxidized PPy/ATP membranes (5 and 10 μm) was studied in phosphate buffer between pH 4.5 and 13 after 5−20 min of equilibration in the corresponding solutions. It was observed that, up to pH = 9, the equilibrium potential was reached quickly (less than 5 min), and the E−pH behavior was quite reproducible and linear ($R > 0.995$) with a Nernstian slope of -60 ± 10 mV/pH, in agreement with eq 5. Between pH = 9 and 13, the apparent slope calculated from the pseudo-equilibrium potentials, as measured after 20 min of equilibration, was about 100 mV/pH and corresponded to eq 6. This deviation from ideality could be due to a shift from equilibrium, since the slow deprotonation process occurrs to a larger extent in this pH range. Further deprotonation of P should also be considered and would result in structural degradation due to radical anion formation.[20]

Spectroscopy. To confirm the trends observed in the potentiometric study, absorption changes of 0.1−0.5 μm thick oxidized PPy/ATP membranes in 0.1 M NaCl were qualitatively evaluated after immersion of the membrane in 1 M N_2H_4, 1 M DTT, or 0.1 M NaOH for 5−20 min. In the case of N_2H_4 (shown in Figure 5A) and DTT reduction, the characteristics of the spectra after treatment matched that for an electrochemically reduced membrane. In agreement with the potentiometry results, the changes were completed more quickly for N_2H_4 than for DTT. Analysis of these spectral changes indicates that both 650 and 400 nm would be suitable working wavelengths for an optical sensor of N_2H_4, DTT, or some other biological reductant.

Upon treatment of oxidized PPy/ATP by NaOH, the interband transition was significantly increased in intensity (above the

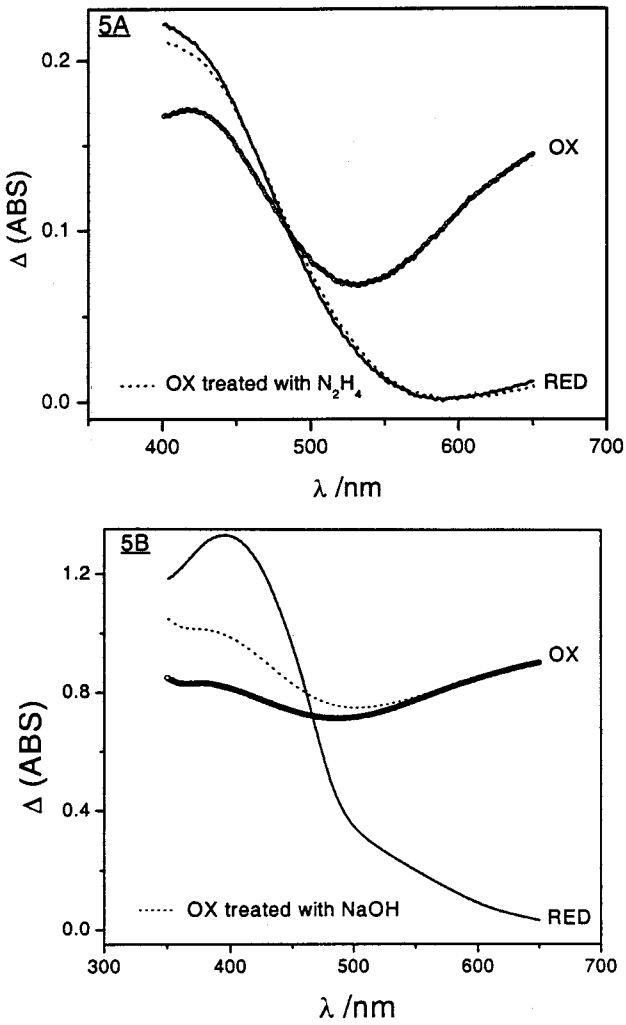

Figure 5. (A) Effect of chemical reduction on the absorbance of a 0.1 μm thick PPy/ATP membrane in 0.1 M NaCl (- - -, oxidized polymer previously treated (10 min) with 1 M N_2H_4; see for comparison the absorbance of the polymer electrooxidized at +0.4V (○) and electroreduced at −0.7 V (—)). (B) Effect of pH on the absorbance of a 0.5 μm thick PPy/ATP membrane in 0.1 M NaCl (- - -, oxidized polymer previously treated (20 min) with 0.1 M NaOH).

−0.3 V electrochemically reduced level) due to neutralization of the charge carriers. At the same time, the low-energy absorption band remained unchanged (Figure 5B). This may be attributed to remaining carriers or to the formation of a more highly conjugated neutral structure with a quinoid-type structure[36] (see structure P in Figure 3). Subsequent acid treatment decreased the intensity of the high-energy transition, in agreement with the injection of new charge carriers. The low-energy band concomitantly decreased in intensity, probably due to structural degradation.

Conductometry. The change of conductivity of PPy/ATP membranes deposited on an IME was studied as a function of N_2H_4 content in the exposure solution. A typical conductometric titration curve (given in terms of I_D) is shown in Figure 6A. The results were reproducible, and the average slope from several experiments was approximately 3 mS per decade of concentration. The response time of the sensor was a function of the film thickness varying from about 10 min for a 5−10 μm thick membrane to 20 min for a 10−15 μm thick membrane, in agreement with a diffusion-limited process for N_2H_4 through the membrane.

Increasing the concentration of N_2H_4 up to 0.1 M, the polymer reduction was found to be quite reversible since more than 90%

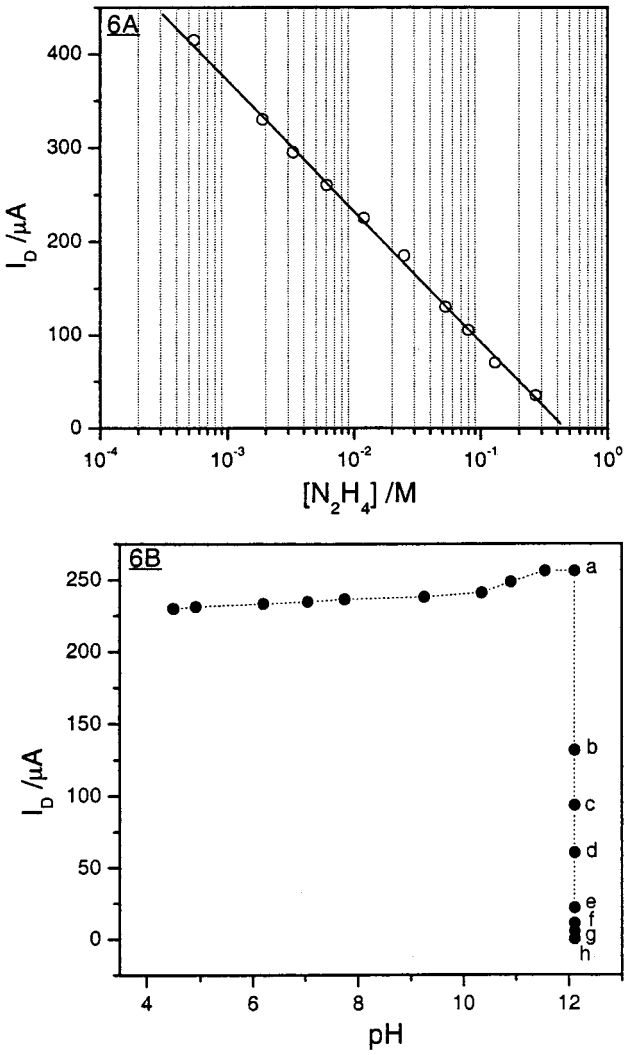

Figure 6. Drain current recorded on a 15 μm thick PPy/ATP membrane IME sensor exposed to a 0.1 M NaCl solution as a function of (A) N_2H_4 content (offset = 50 mV) and (B) pH (offset = 30 mV). The measurements were carried out after 5 min equilibration for pH 4−12 and then at a = 0.1, b = 3, c = 6, d = 9, e = 12, f = 15, g = 18, and h = 20 min after pH = 12 exposure.

of the conductivity could be recovered by reoxidation with an Fe(III) salt. Furthermore, immersion of the film in 0.1 M HCl led to a similar result and even a higher conductivity in strongly acidic medium (0.5 M H_2SO_4). This higher conductivity suggests that a significant amount of deprotonation of the oxidized polymer by N_2H_4 may be occurring (note that a solution of 0.1 M N_2H_4, 0.1 M NaCl has a pH = 10.5), and the strong acid serves to compensate for this effect while also protonating the pyrroles to a high degree.

A study of the in-situ conductivity of 10 μm thick membranes of PPy/ATP in an alkaline medium confirmed the sluggishness of the deprotonation process. As seen in Figure 6B, the conductivity (measured 5 min after each NaOH addition in the buffer medium) did not change significantly up to pH = 12. This is in contrast to other reports indicating a sigmoidal relationship between conductivity and pH with a 2 orders of magnitude change between pH 3 and 11.[9] Recent work has also indicated no dopant extraction for a PPy composite between pH 2 and 11.[37] Above pH 12, we observed a sharp decrease in conductivity, though the process was slow (30 min to reach negligible conductivity, see points a−g in Figure 6B). Overall, the deprotonation process remained quite reversible below pH = 12, and complete recovery of the conductivity was observed after immersion of the film in 0.1 M HCl.

The results outlined above indicate that a PPy membrane could be used to sense a chemical species using a number of physical chemical parameters including electrical conductivity, electrode potential, and optical absorption. No selectivity was expected here, nor was a high sensitivity for our sensors. The first issue could be addressed by chemical functionalization of the polymer, while the second could be addressed with an appropriate design of the membrane/IME's.

Study of Electrochemically Triggered Release of ATP. As mentioned in the Introduction, when considering this type of conducting polymer as a delivery system, the anionic drug is incorporated during electrosynthesis and remains electrostatically bound to the polymer inside the membrane. The application of a negative potential neutralizes the positive charges on the polymer and allows the drug to diffuse out of the membrane. While the release of ATP from PPy/ATP was reported earlier,[6] here we more fully detail the parameters that control this process and model the mass transport properties in these membranes.

Electrochemical Parameters of Release. Typical spectroscopic and electrochemical results for a release experiment carried out at $E = -0.7$ V on a 10 μm thick PPy/ATP membrane are presented in Figure 7. The absorbance due to ATP being emitted into the supporting electrolyte in contact with the membrane is seen to increase with release time as shown in Figure 7A. Release of ATP from the membrane was found to be a rather slow process (more than 10 min for completion, curve b), in contrast to the electrochemical reduction process. The normalized chronocoulogram shown in Figure 7B shows that, in less than 60 s, about 300 mC cm^{-2} was injected into the polymer corresponding to 0.25 e^-/pyrrole (assuming no significant contribution from underlying electrode).

Attempts to model the current with the Cottrel equation failed, indicating that the electrochemical reduction of PPy/ATP did not follow a simple diffusional model. This is likely due to structural changes that occur in the polymer during redox switching and the multiionic nature of the dopant which complicates the analysis.[3a] As evidenced in Figure 7B, only very small quantities of ATP were optically detected in the NaCl solution at the stage where most of the electrochemical reduction had occurred. This is due to the fact that the charge was mainly balanced by Na^+ insertion as shown in previous electrochemical quartz crystal microbalance (EQCM) experiments.[6a] As will be shown below, the ATP release process likely occurs through diffusion of $ATP^{3-}Na^+_3$ ion aggregates and was polymer structure (membrane porosity) dependent. No significant release occurred above a given gate potential (about −0.3 V), and the mass transfer rate increased as a function of gate potential from −0.4 to −0.8 V. For a given structure, this suggested that the electrical potential could induce a structural effect due to pore opening related to initial cation insertion. It is interesting to note that slow potential cycling allowed a higher ATP release rate than did a large step potential. In addition, a PPy/ATP membrane first cycled in ATP solution exhibited faster (near immediate) release when compared to an as-made membrane. In both cases, this is probably due to the pore-opening process. The total amount of ATP released could also be adjusted by controlling the exposed area of the membrane and its thickness (between 0.1 and 50 μm for an electrochemically deposited membrane) providing the polymer remained electroactive.

The effect of current density used for polymer synthesis was studied between 0.1 and 10 mA cm^{-2}. Using an absorbance

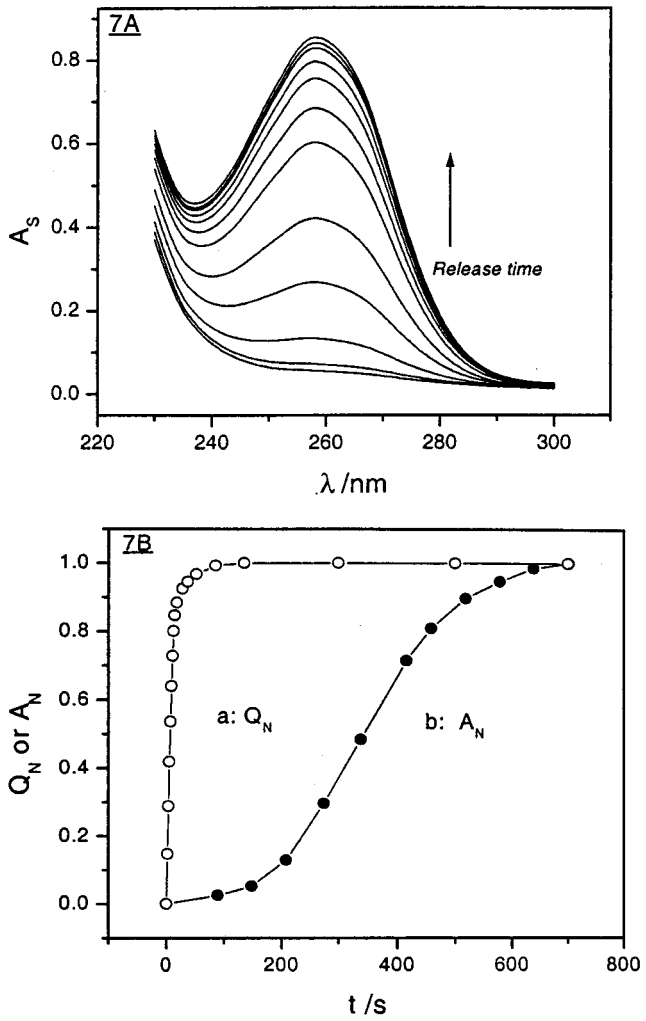

Figure 7. (A) Absorbance spectra of a 0.1 M NaCl solution (A_S) in contact with a 10 μm thick PPy/ATP membrane subjected to a release potential of −0.7 V. (B) Normalized absorbance of ATP at 260 nm (A_N) in the contact electrolyte (curve b) and electrochemical charge modulus Q_N (curve a) during the release experiment described in (A).

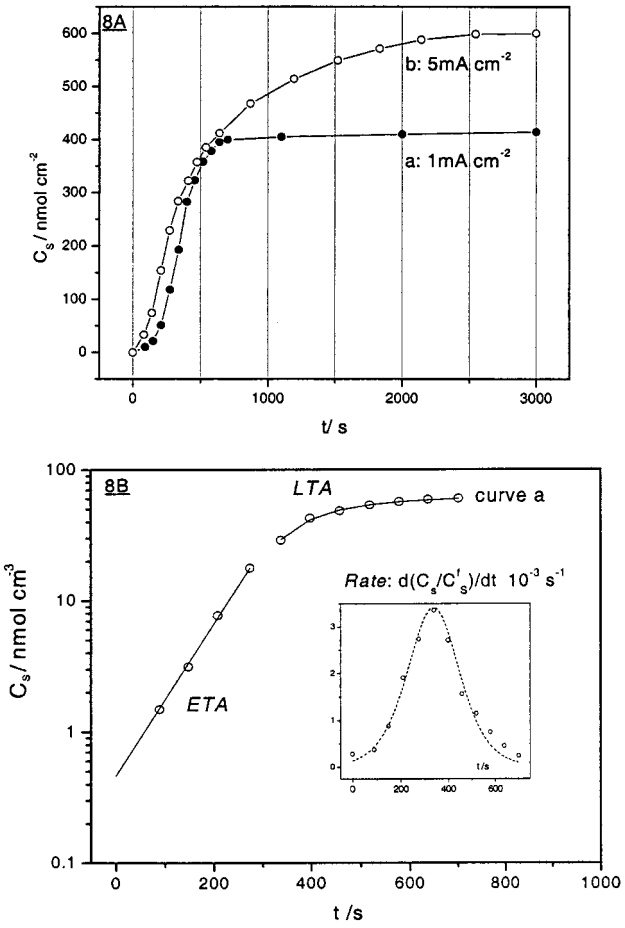

Figure 8. (A) Concentration of ATP (C_s) as a function of time (release profile) in a 0.1 M NaCl solution in contact with a 10 μm thick PPy/ATP membrane electrosynthesized at (curve a) 5 mA cm^{-2} and (curve b) 1 mA cm^{-2}. (B) Curve a: concentration of ATP (C_s) as a function of time for the dense membrane showing the fitting curves (—) for both early (ETA) and late (LTA) time approximates (from respectively eqs 11 and 12 in the text). Curve b (frame): rate of delivery as a function of time of release derived from curve a (dot plot is only indicative).

calibration curve obtained from ATP standard concentration solutions ($A_S(260) = 14174$[ATP], $R = 0.999$), the amount of ATP released was evaluated. As illustrated in Figure 8A, for membranes synthesized with a low polymerization rate (0.1−1 mA cm^{-2}), the amount released was approximately 400 nmol cm^{-2} (∼0.2 e$^-$/pyrrole ring in the polymer), while for membranes electrosynthesized at a higher rate (above 5 mA cm^{-2}), the amount released was closer to 600 nmol cm^{-2} (∼ 0.25 e$^-$/ring). We believe that the release differences arise from a trapping of ATP in the *dense* membranes made at low current densities, while the higher porosity material would facilitate the diffusion of more ATP. The mean transfer rate of ATP could also be estimated from the release profiles and gave 35 nmol cm^{-2} min^{-1} (18 μg cm^{-2} min^{-1}) for the *dense* membrane (curve b, Figure 8A) and only 15 nmol cm^{-2} min^{-1} (8 μg cm^{-2} min^{-1}) for the *porous* membrane (curve a, Figure 8A). This demonstrates that complete emission of the drug is a slow process. Both of these parameters (total amount and mean rate of delivery) define the basic characteristics of the drug delivery system. To better understand and predict the release rate of the delivery system, we have modeled the kinetics of the release process.

Release Modeling. Drug release from polymeric delivery systems has been modeled for a variety of devices and geometries.[1a] Although our system can be identified as matrix type (monolithic), the drug loading process gives it unique properties. As can be seen in Figure 8A, the release profiles are characterized by slow kinetics at the early times ($t < 5$ min), followed by a sharp increase in the delivery rate later. Interestingly, the time function dependence was of square root type for *porous* membranes, whereas a sigmoidal function characterized the *dense* membranes behavior.

Since a better reproducibility of the release profiles was achieved with the denser membranes, mass transport modeling was performed on these. A simple transport model was chosen assuming a pure diffusion process within a constant diffusion layer equal to the membrane thickness (L). Using Fick's first law in its linearized form, the drug flux (J) out of the membrane is expressed as

$$J = -D(C_{is} - C_{ie})/L \qquad (7)$$

where D is the apparent diffusion coefficient of ATP, and C_{is} and C_{ie} are the concentration of ATP at the membrane/solution interface (is) and membrane/electrode interface (ie), respectively. The flux of ATP into the solution is then written as a function

of time as

$$J = A\, dC_s/dt \tag{8}$$

where C_s is the bulk concentration of ATP in solution and A is the exposed area of the membrane. Making the flux equal from eqs 7 and 8, the following diffusion differential equation is obtained:

$$dC_s/[C_s - (C^0{}_M - C_{is})/K_V] = (-2D/L^2)t \tag{9}$$

where $C^0{}_M$ is the initial concentration of ATP in the membrane, and $K_V = V_S/V_M$, with V_S and V_M being the solution and membrane volumes, respectively. This equation is deduced knowing that the total amount of ATP distributed between membrane and solution is constant and also assumes that the mean concentration of ATP in the membrane is a linear average between C_{is} and C_{ie}. To solve the differential equation and deduce C_s as a function of time, other conditions with respect to the concentration of ATP are required. Since the release rate profile was found to be of a Gaussian type (symmetrical with a maximum at half time, see curve b in Figure 8B), two regimes of diffusion were considered and early (ETA) and late (LTA) time approximations were introduced to solve the diffusion equation. We believe that the physics associated with this unusual behavior arises from the inhibited diffusion process that occurs due to initial pore restriction in the first step of the release. It is worth noting that, in the case of a more porous membrane (curve b, Figure 8a), the release rate decreases constantly as expected for a unchanging pore size. For ETA, C_{ie} was considered constant and equal to $C^0{}_M$; under these conditions, it can be easily shown that

$$C_{is} = C^0{}_M - 2K_V C_s \tag{10}$$

Substituting in eq 9 and integrating, the time-dependent function of C_s was deduced:

$$C_s = \exp[(2D/L^2)t] \tag{11}$$

A good fit of the experimental data was obtained with this equation up to 300 s of time release ($R = 0.998$) and gave a value of 6.7×10^{-9} cm^2 s^{-1} for D (see Figure 8B, curve a, ETA part). For LTA, although C_{is} could be considered as equal to the final concentration of ATP in the membrane ($C^f{}_M$), the final portion of the curve was fit allowing the unknown parameters to float which led to the following equation:

$$C_s = (C^0{}_M - C_{is})/K_V + [C_s(t^0) - (C^0{}_M - C_{is})/K_V] \exp[(-2D/L^2)(t - t^0)] \tag{12}$$

Here again, a consistent fit was achieved ($R = 0.998$), initializing for $t^0 = 338$ s. The identification of the first unknown parameter gave 2.15×10^{-4} mol cm^{-3} for C_{is}, which was in excellent agreement with $C^f{}_M$ (calculated equal to be 2.30×10^{-4} M from the final concentration in solution $C^f{}_S$), and the last parameter gave 4.0×10^{-9} cm^{-2} s^{-1} for D (see Figure 8B, curve a, LTA part). It can be seen that the apparent diffusion coefficient of ATP during the release process, as determined by our method, is roughly constant. The small differences are likely due to the two additional physical processes [initial pore restriction and late ionic hindrance ($C^f{}_M \sim 25\%\ C^0{}_M$)] associated with the diffusion process. The value of ATP diffusivity in these polypyrrole membranes was found to be intermediate between solvent swollen rubbery and glassy polymers used in polymeric drug delivery devices.[1a] However, the diffusivity of ATP could be easily enhanced by tailoring the polymer morphology; indeed, the polymeric system could comprise an inner porous reservoir layer (obtained by high rate polymerization) and an external thin dense layer to avoid spontaneous release. On the other hand, drug delivery with this type of system could be adjusted as desired by electrochemical triggering. This mode of control would allow a pulsatile release with an adjustable rate either by using gate potential control (the rate can change from 0 to 100% according to the potential value) or by individually addressing microreservoirs patterned in the membrane.[38]

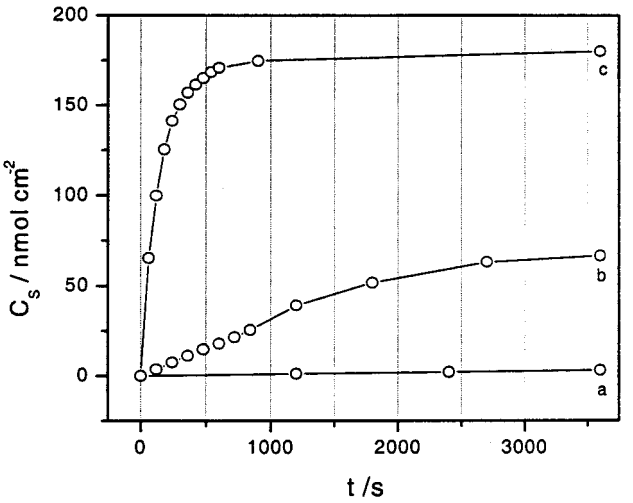

Figure 9. Concentration of ATP in solution (C_s) as a function of time in contact with a 10 μm thick membrane PPy/ATP. The solution is (a) 0.1 M NaCl, (b) 0.1 M NaCl/0.1 M N_2H_4, and (c) 0.1 M NaCl/0.1 M NaOH.

To summarize this section, we have shown that a controlled ATP delivery system can be achieved by adjusting both polymer synthesis and electrochemical release parameters. Further, we can predict the release rate based on a simple diffusional model.

Study of Chemically Triggered ATP Release. To bring the chemical sensing and externally stimulated release characteristics together, we investigated the chemically induced (reductive or alkaline stimuli) release characteristics of PPy/ATP. It was first confirmed that the absorbance ($\lambda_{max} = 260$ nm) of 10^{-5} M ATP was stable to N_2H_4, DTT, and alkaline environmental exposure. No apparent chemical change occurs either when DTT or N_2H_4 was added up to concentrations of 10^{-1} M or the pH was increased up to 12.

ATP Release by N_2H_4. As illustrated by curve a in Figure 9, a very low amount of spontaneous release occurred when a freshly prepared ATP loaded membrane was exposed to 0.1 M NaCl; indeed, for a period of 2−3 days, the spontaneous release was less than 5%. The absorbance of the 0.1 M NaCl bathing solution was then monitored as successive increments of N_2H_4 (10 mM) were added under constant stirring. It was observed that the absorbance increased slowly after each addition, with about 20 min required to stabilize the solution absorbance for a 10 μm thick membrane. These results strongly support the diffusion-controlled release of the ATP from the membrane. Complete release of ATP was reached at about 0.1 M N_2H_4; continued ATP release did not occur with further N_2H_4 addition up to 1 M.

The amount of ATP released as a function of time in 0.1 M N_2H_4/0.1 M NaCl solution is shown in Figure 9 (curve b). As expected, the release kinetics were slower than that for the electrochemical process (compare with curve b, Figure 7B) as two species are required to diffuse (N_2H_4 in and ATP out), and

the membrane has a less porous structure (no ionic exchange occurred initially as with the electrochemical process).

It should be noted that the maximum amount of ATP that could be released chemically was about 70 nmol cm^{-2} (0.5 μg cm^{-2} min^{-1}), which is less than 20% of the amount released electrochemically. This may be due to ATP entrapment within the PPy membrane or incomplete reaction of N_2H_4 with PPy/ATP.

ATP Release vs DTT. No measurable ATP release could be detected for a PPy/ATP membrane exposed to a 0.05 M DTT/0.1 M NaCl solution for up to 1 h. However, this experiment could not be taken as conclusive due to experimental difficulties (strong background absorbance of DTT) and slow kinetic processes involved in the release.

ATP Release vs pH. The release of ATP induced by a 0.1 M NaOH/0.1 M NaCl solution is shown to be a fast process in Figure 9, curve c. Here the release is associated with the chemical deprotonation of PPy and the diffusion of ATP out of the film. Surprisingly, the ATP release maximum was reached in a shorter time than that observed with electrochemical triggering, and the release profile showed characteristics of zero-order kinetics.[1a] However, in contrast to small counteranion dopants that can be totally extracted by alkaline treatment,[25] significant entrapment of ATP is also observed here where only about 40% of the electrochemically released amount was detected. Specifically, the basic trigger released 175 nmol cm^{-2} (6 μg cm^{-2} min^{-1}). In addition to the reasons given above for N_2H_4-induced release, the possibility of ion pairing of ATP−Na may be a factor.

Final Discussions and Conclusion

The simple polymer/drug model we have employed in this work demonstrates that it is possible to build a controlled release device based on a conductive electroactive polymer in a number of different configurations. By adjusting the structural and geometrical parameters of the active membrane, nanogram to milligram amounts of ATP could be released using this methodology. For example, a 5 cm diameter by 50 μm thick disk would contain 40 mg of ATP. Delivery rates can be controlled from minutes to hours using chemical methods, while electrochemical release methods provide even further flexibility. Using multicoating polymer systems, codelivery of drugs would be possible by choosing selective redox potential and/or ion-transporting polymers.[39]

In the future, conducting polymers based biomedical devices will likely find specific therapeutic applications as bioanalytical microelectrodes or for in-vivo drug delivery.[40] One other important point to be considered in a drug delivery system is its biocompatibility. Conducting polymers based on PPy have low cytotoxicity[21] and are stable to a broad selection of redox and acid/base conditions. Further, Reynolds et al. have recently reported on aqueous compatible polypyrrole derivatives [poly-(3,4-ethylenedioxypyrrole) (PEDOP)] which exhibit even further stability to reduction than its parent PPy.[41]

More generally, we have shown that the characteristics of the diffusing species and the structure of the polymer matrix allows some prediction of the kinetics of release and could yield guidelines for the development of new drug delivery systems. As already reported,[6b] PPy-based systems are well-behaved for anionic drug release. The drug-loaded membranes were easily handled, were quite stable in air, and demonstrated low spontaneous release in aqueous medium for a long period. The release of ATP ions from PPy membranes using chemical triggers including hydrazine (0.1 M) and alkaline media (NaOH 0.1 M) was quantified for the first time here, demonstrating a self-regulated drug delivery device. Using spectrophotometric monitoring of drug concentration in a solution in contact with a loaded membrane, the diffusion of ATP through the polymer membrane was modeled, and a diffusion coefficient close to 5×10^{-9} cm^2 s^{-1} was calculated for ATP in the case of electrochemical triggering. The chemical sensing of N_2H_4 by PPy membranes was quantified using potentiometric and conductometric titration, and a linear response with concentration logarithm was obtained in the range 10^{-4}−1 M.

Acknowledgment. Financial support from the National Science Foundation (CHE 96-29854) is greatly appreciated. J.M.P. acknowledges UFMG and CAPES, Brasilia/Brazil. We also thank Katherine Williams from Department of Chemistry/UF, who made CCD spectrophotometric measurements possible.

References and Notes

(1) (a) Park, K., Ed. *Controlled Drug Delivery, Challenges and Strategies*; American Chemical Society: Washington, DC, 1997. (b) Langer, R. *Science* **1990**, *249*, 1527.

(2) (a) Robinson, J. K., Vincent, H. L. L., Eds. *Controlled Drug Delivery, Fundamentals and Applications*, 2nd ed.; Marcel Dekker: New York, 1987. (b) Uhrich, K. E.; Cannizarro, S. M.; Langer, R. S.; Shakesheff, K. M. *Chem. Rev.* **1999**, *99*, 3181.

(3) (a) Lyons, M. E. G., Ed. *Electroactive Polymer Electrochemistry, Part 1 Fundamentals*; Plenum Press: New York, 1994. (b) Skotheim, T. A., Elsenbaumer, R. L., Reynolds, J. R., Eds. *Handbook of Conducting Polymers*, 2nd ed.; Marcel Dekker: New York, 1998.

(4) Chang, A. C.; Miller, L. L. *J. Electroanal. Chem.* **1988**, *247*, 173.

(5) Zinger, B.; Miller, L. L. *J. Am. Chem. Soc.* **1984**, *106*, 6861.

(6) (a) Pyo, M.; Maeder, G.; Kennedy, R. T.; Reynolds, J. R. *J. Eectroanal. Chem.* **1994**, *368*, 329. (b) Pyo, M.; Reynolds, J. R. *Chem. Mater.* **1996**, *8*, 128.

(7) (a) Zhou, Q. X.; Miller, L. L.; Valentine, J. R. *J. Electroanal. Chem.* **1989**, *261*, 147. (b) Reynolds, J. R.; Ly, H.; Selampinar, F.; Kinlen, P. J. *Polym. Prepr.* **1999**, *40*, 307.

(8) (a) Burgmayer, P.; Murray, R. W. *J. Am. Chem. Soc.* **1982**, *104*, 6139. (b) Stassen, I.; Sloboda, T.; Hambitzer, G. *Synth. Met.* **1995**, *71*, 2243. (c) Zhao, H.; Price, W. E.; Wallace, G. G. *J. Membr. Sci.* **1998**, *148*, 161.

(9) (a) Guiseppi-Elie, A.; Wallace, G. G.; Matsue, T. Chemical and biological sensors based on electrically conducting polymers. In ref 3b; Chapter 34. (b) Swager, M. T. *Acc. Chem. Res.* **1998**, *31*, 201.

(10) (a) Bartlett, P. N.; Cooper J. M. *J. Electroanal. Chem.* **1993**, *362*, 1. (b) Sargent, A.; Thomas, L.; Susannah, G.; Sadik, O. A. *J. Electroanal. Chem.* **1999**, *470*, 144.

(11) Cunningham, A. J. *Introduction to Bioanalytical Sensors*; John Wiley & Sons: New York, 1998.

(12) Chiang, C. K.; Fincher, Jr., C. R.; Park, Y. W.; Heeger, A. J.; Shirakawa, H.; Louis, E. J.; Gau, S. C.; MacDiarmid, A. G. *Phys. Rev. Lett.* **1977**, *39*, 1098.

(13) Ratcliffe, N. M. *Anal. Chim. Acta* **1990**, *239*, 257.

(14) Hanawa, T.; Yoneyama, H. *Synth. Met.* **1989**, *30*, 341.

(15) Lu, Z.; Sun, Z.; Dong, Z. *Electroanalysis* **1989**, *1*, 271.

(16) Paul, E. W.; Ricco, A. J.; Wrighton, M. S. *J. Phys. Chem.* **1985**, *89*, 1411.

(17) Foul, N. C.; Lowe, C. R. *J. Chem. Soc., Faraday Trans. 1* **1986**, *82*, 1259.

(18) Livache, T.; Roget, A.; Dejean, E.; Barthet, C.; Bidan, G.; Theoule, R. *Nucl. Acids Res.* **1994**, *22*, 2915.

(19) Sadik, O.; Wallace, G. *Anal. Chim. Acta* **1993**, *279*, 209.

(20) Genies, E. M.; Syed, A. A. *Synth. Met.* **1984**, *10*, 21.

(21) (a) Wong, J. W.; Langer, R.; Ingber, D. E. *Proc. Natl. Acad. Sci. U.S.A.* **1994**, *91*, 3201. (b) Schmidt, C. E.; Shastri, V. R.; Vacanti, J. P.; Langer, R. *Proc. Natl. Acad. Sci. U.S.A.* **1997**, *94*, 8948. (c) Garner, B.; Hodgson, A. J.; Wallace, G. G.; Underwood, P. A. *J. Mater. Sci. Mater. Med.* **1999**, *10*, 19.

(22) Somlo, E. *Lancet* **1955**, *268*, 1125.

(23) Ellis, D. L.; Zakin, M. R.; Bernstein, L. S.; Rubner, M. F. *Anal. Chem.* **1996**, *68*, 817.

(24) Lamoureux, G. V.; Whitesides, G. M. *J. Org. Chem.* **1993**, *58*, 633.

(25) Inganas, O.; Erlandsson, R.; Nylander, C.; Lunstrom, I. *J. Phys. Chem. Solids* **1984**, *45*, 427.

(26) Pernaut, J. M.; Genies, E. M. *Synth. Met.* **1984**, *10*, 117.

(27) Paul, E. W.; Ricco, A. J.; Wrighton, M. S. *J. Phys. Chem.* **1985**, *89*, 1441.

(28) Boyle, A.; Genies, E.; Fouletier, M. *J. Electroanal. Chem.* **1990**, *279*, 179.
(29) Zotti, G. *Synth. Met.* **1998**, *97*, 267.
(30) Pei, Q.; Qian, R. *Electrochim. Acta* **1992**, *37*, 1075.
(31) Petek, M.; Bruckenstein, S. *J. Electroanal. Chem.* **1973**, *47*, 329.
(32) Harrison, J. A.; Khan, Z. A. *J. Electroanal. Chem.* **1970**, *28*, 131.
(33) Vieil, E.; Pernaut, J. M.; Genies, E.; Nechtschein, M.; Devreux, F.; Genoud, F. *Synth. Met.* **1986**, *15*, 59.
(34) Jocelyn, P. C. *Biochemistry of the SH Group;* Academic Press: New York, 1972.
(35) Munstedt, H. *Polymers* **1986**, *27*, 899.
(36) (a) Tan, K. L.; Tan, B. T. G.; Kang, E. T.; Neoh, K. G. *J. Chem. Phys.* **1991,** *94*, 5382. (b) Pei, Q.; Qian, R. *Synth. Met.* **1991**, *45*, 35.
(37) Chen, Z.; Okimoto, A.; Kiyonaga, T.; Nagaoka, T. *Anal. Chem.* **1999**, *71*, 1834.
(38) Santini Jr., J. T.; Cima, M. J.; Langer, R. *Nature* **1999**, *397*, 335.
(39) Pyo, M.; Reynolds, J. R. *J. Phys. Chem.* **1995**, *99*, 8249.
(40) Pito, B.; Pham, M. C.; Ledoan, T. *J. Biomed. Mater. Res.* **1999**, *46*, 566.
(41) Thomas, C.; Zhong, K.; Schottland, P.; Reynolds, J. R. *Adv. Mater.* **2000**, *12*, 222.